Journal of Applied Physics

Edge effects on the high-frequency dynamics of Dzyaloshinskii domain walls

Cite as: J. Appl. Phys. **126**, 163904 (2019); https://doi.org/10.1063/1.5124316
Submitted: 13 August 2019 • Accepted: 10 October 2019 • Published Online: 25 October 2019

Mao-Kang Shen, Yue Zhang, Zai-Dong Li, et al.

AIP Publishing

Journal of Applied Physics ARTICLE scitation.org/journal/jap

Edge effects on the high-frequency dynamics of Dzyaloshinskii domain walls

Cite as: J. Appl. Phys. **126**, 163904 (2019); doi: 10.1063/1.5124316
Submitted: 13 August 2019 · Accepted: 10 October 2019 ·
Published Online: 25 October 2019

Mao-Kang Shen,[1] Yue Zhang,[1] Zai-Dong Li,[2,3] Long You,[1] Wei Luo,[1] and Xiao-Fei Yang[1]

AFFILIATIONS

[1]School of Optical and Electronic Information, Huazhong University of Science and Technology, Wuhan 430074, People's Republic of China
[2]Department of Applied Physics, Hebei University of Technology, Tianjin 300401, People's Republic of China
[3]School of Science, Tianjin University of Technology, Tianjin 300384, People's Republic of China

Author to whom correspondence should be addressed: yue-zhang@hust.edu.cn

ABSTRACT

Chiral domain walls (DWs) in perpendicularly magnetized nanotracks (PMNTs) with interfacial Dzyaloshinskii-Moriya interaction (DMI) have become the primary objects of theoretical and experimental investigation due to their technological suitability in spintronic nanodevices. In this work, sway mode, a periodic dislocation of DWs, is found in a PMNT with a strong DMI under a high-frequency out-of-plane alternating magnetic field using micromagnetic simulation. This sway mode is out of prediction by the traditional collective coordinate method without considering edge effects. It is originated from DMI-related antisymmetric tilting of moments at two track edges, which results in inhomogeneous precession of moments throughout the DW under an out-of-plane alternating magnetic field. This work demonstrates the important role of edge effects to the dynamics of DWs with a strong DMI.

INTRODUCTION

Physical mechanism and manipulation of domain walls (DWs) motion in magnetic nanotracks have been extensively investigated over the last few decades, driven by scientific interest and potential applications in high-performance spintronic devices. The DW motion can be triggered by a static or alternating magnetic field,[1–4] spin transfer torque,[5–14] spin-orbit torque (SOT),[15–27] electric field,[21,28–31] spin waves (magnons),[32–37] etc. In recent years, theoretical and experimental studies have revealed the crucial role of interfacial Dzyaloshinskii-Moriya interaction (DMI) in the structure and dynamics of a chiral Néel-type DW in heavy metal (HM)/ferromagnet (FM) heterostructures.[16–21,29–31,38,39] For instance, it is widely observed that the DW plane with strong DMI tilts under current-induced SOT.[22–27]

In theory, DW dynamics has been widely studied by the collective coordinate method (CCM) that always takes DW as a rigid body whose motion is depicted by the dynamic equations of several collective coordinates.[40–42] However, this rigid-body assumption seems not quite applicable to the DW dynamics under strong DMI. Very recently, Slastikov *et al.* have investigated the effects of a static magnetic field on the DW motion with DMI beyond the CCM.[43] On the other hand, because of the DMI-induced edge effect, the DW also exhibits a much more complicated dynamic behavior.[26,44–46]

In this study, we show a novel sway mode for DWs in perpendicularly magnetized nanotracks (PMNTs) with a strong DMI under an out-of-plane high-frequency alternating magnetic field based on micromagnetic simulation. This sway mode is originated from the DMI-relevant edge effects that result in an inhomogeneous precession of moments throughout the DW plane.

SIMULATION METHOD

The DW motion driven by an alternating magnetic field was simulated using the software named "Object-Oriented Micro-Magnetic Framework" (OOMMF) with the code of interfacial DMI.[47] We consider a long track with perpendicular magnetic anisotropy (PMA) and the dimension $2000 \times 100 \times 0.6\,\mathrm{nm}^3$, and the cell dimension is $2 \times 1 \times 0.6\,\mathrm{nm}^3$. The parameters include

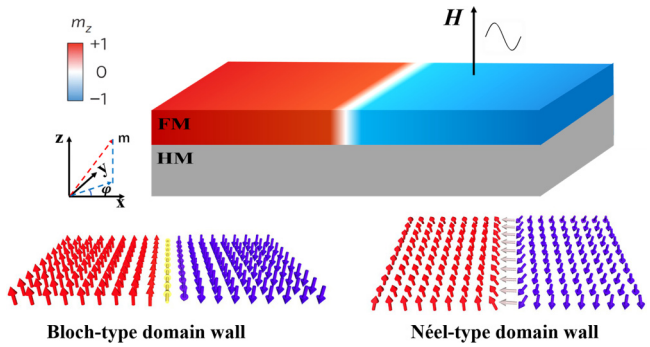

FIG. 1. (a) Schematic of the sway of a chiral DW under an out-of-plane alternating magnetic field in an FM/HM bilayer; (b) Bloch-type DW without DMI and the Néel-type DW with a negative DMI constant.

the saturation magnetization $M_S = 7 \times 10^5$ A/m, the exchange stiffness constant $A = 1 \times 10^{-11}$ J/m, the anisotropy constant $K = 4.8 \times 10^5$ J/m^3, and the damping coefficient $\alpha = 0.03$ or 0.002. The smaller α is used for a Fast Fourier Transformation (FFT). When the DMI constant (D) is zero, the initial DW exhibits a Bloch-type structure (down left in Fig. 1). However, when D varies from -0.05 mJ/m^2 to -1.5 mJ/m^2, the DW changes to a Néel-type one with a left-handed chirality (down right in Fig. 1).

To determine the characteristic frequency of DW dynamics, the initial equilibrium state of DW was perturbed by an out-of-plane alternating magnetic field as a sinc function of time,

$$\vec{h}(t) = h_{\max}\mathrm{sinc}[2\pi f_c(t - t_0)]\vec{e}_z, \tag{1}$$

where

$$\mathrm{sinc}\,[2\pi f_c(t - t_0)] = \begin{cases} \dfrac{\sin[2\pi f_c(t - t_0)]}{2\pi f_c(t - t_0)}, & t \neq t_0, \\ 1, & t = t_0, \end{cases} \tag{2}$$

with $t_0 = 0.25$ ns, $f_c = 20$ GHz, and $h_{\max} = 10$ mT. The excitement lasts for 0.5 ns. The data were collected 2 ns after finishing the excitement to avoid nonlinear terms.

The equilibrium magnetization (m_0) was removed from the recorded magnetization dynamics. The remaining time-dependent magnetization was transformed into the frequency domain using the FFT with a spatially averaged route,[48]

$$P(f) = \sum_{k=x,y,z} \left| \sum_{j=1}^{n} \langle \Delta m_k(t_j) \rangle e^{-i2\pi f t_j} \right|^2. \tag{3}$$

Here, $\Delta m_k\,(t_j) = m_k\,(t_j) - \,(m_o)_k$, $k = x, y, z$. $t_j = j\Delta t$, where Δt, the time step, is 10 ps and $n = 2000$.

RESULTS AND DISCUSSION

Very weak peaks were detected in the FFT spectra for the 0- or -0.05-mJ/m^2 D [Figs. 2(a)–2(d)]. However, when $D = -1.2$ mJ/m^2, three characteristic frequencies at 0.1 GHz, 1.4 GHz, and 4.35 GHz were found [the peak at 0.1 GHz appears since the 0-GHz alternating magnetic field corresponds to zero magnetic field strength instead of a direct magnetic field; Eqs. (1) and (2)]. On the other hand, the oscillation of m_y and m_z mainly contributes to these peaks. The DW motion under the alternating magnetic fields as a sine function of time

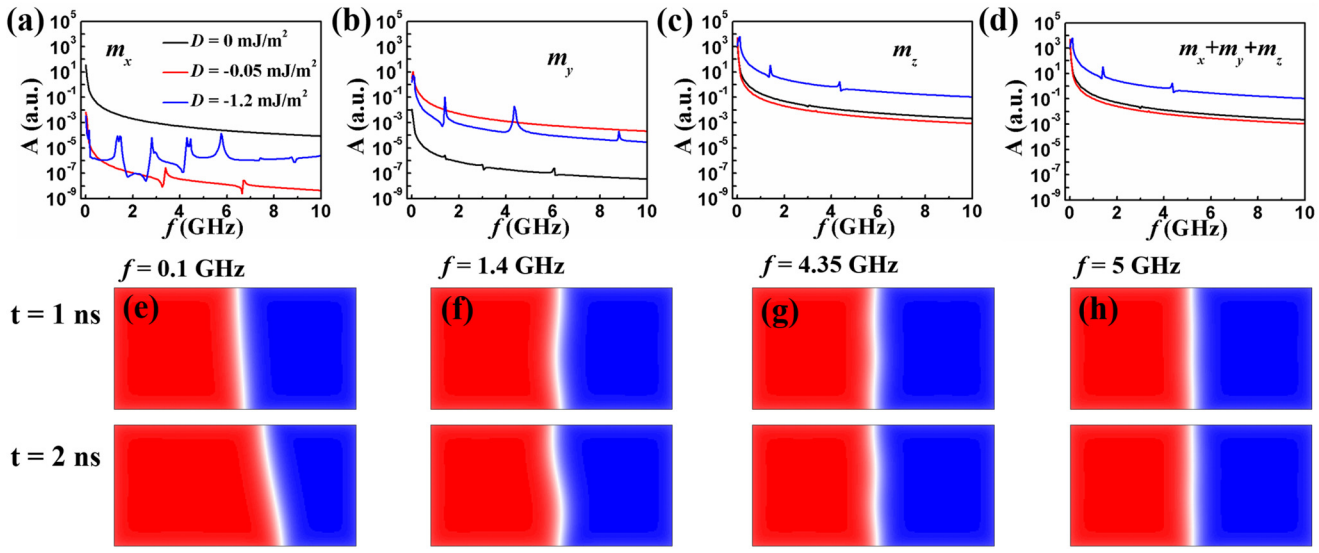

FIG. 2. Dynamics of DWs under out-of-plane alternating magnetic fields. (a)–(d) Contribution of the time-dependent m_x, m_y, m_z, and total m to the FFT spectra in the FM/HM bilayer with different DMI constants. (e)–(h) Snapshots of DWs for $D = -1.2$ mJ/m^2 at different time under sine alternating magnetic fields with different frequencies.

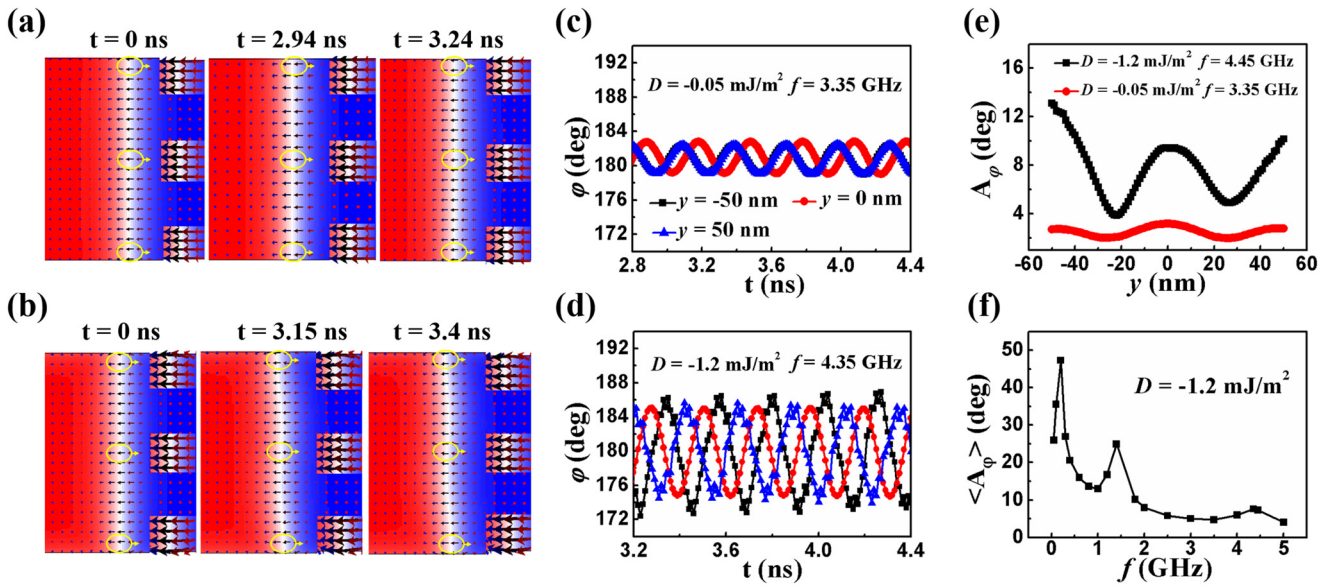

FIG. 3. Temporal distribution of magnetic moments in the DW, driven by the alternating magnetic field for (a) $D = -0.05\ \mathrm{mJ/m^2}$ and (b) $D = -1.2\ \mathrm{mJ/m^2}$. (c) and (d) Oscillation of azimuthal angel φ in the middle of DW at different y coordinates for $D = -0.05\ \mathrm{mJ/m^2}$ and $D = -1.2\ \mathrm{mJ/m^2}$. (e) Variation of the amplitude of φ (A_φ) with y for $D = -0.05\ \mathrm{mJ/m^2}$ and $D = -1.2\ \mathrm{mJ/m^2}$. (f) Frequency spectra of the spatial average of A_φ for $D = -1.2\ \mathrm{mJ/m^2}$.

(the amplitude is 2 mT) at several frequencies was analyzed individually [Figs. 2(e)–2(h)]. When the frequency is as low as 0.1 GHz, the DW plane tilts but keeps almost straight. At 1.4 GHz and 4.35 GHz, the DW deforms periodically and exhibits an S-shape plane. At a very high frequency ($f = 5$ GHz), the DW plane seems to recover to a straight line and moves very slowly (see the movies in the supplementary material for more details).

The DW sways because of distinct local DW velocities at different positions due to the nonuniform precession of moments throughout the DW (Fig. 3). Under an alternating field, the phase and amplitude for the oscillation of azimuthal angle (φ as depicted in Fig. 1) for the moment in DW (A_φ) are not uniform in space [Figs. 3(c)–3(e)]. When D is $-0.05\ \mathrm{mJ/m^2}$, A_φ is smaller than 4°, and A_φ near the track edge is a little smaller than that in

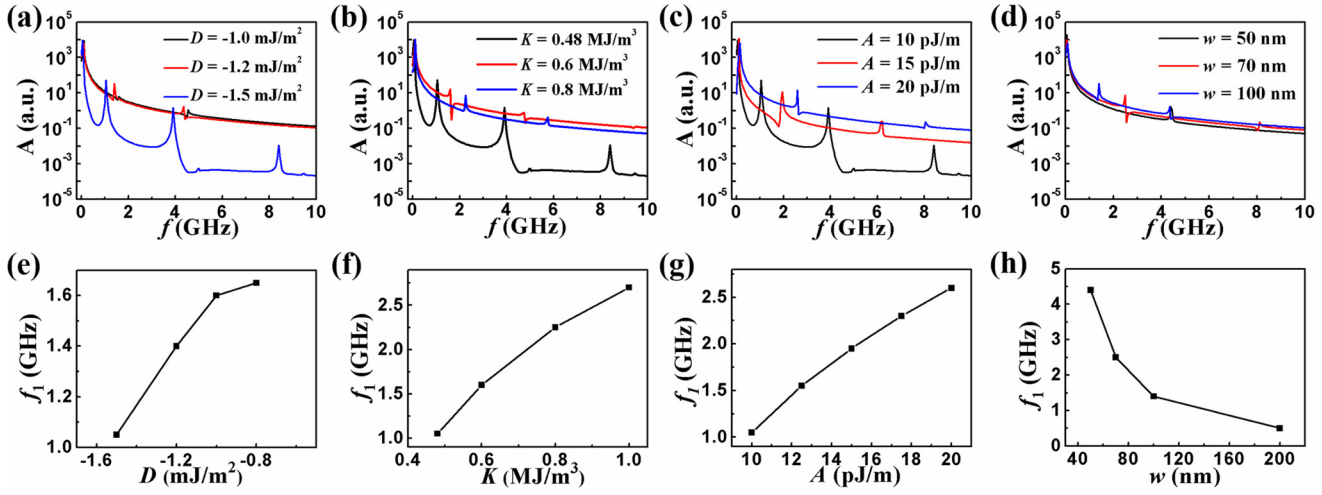

FIG. 4. (a)–(d) FFT spectra of time-dependent magnetization in the FM/HM bilayer track with different DMI constants D, anisotropy constants K, exchange stiffness constants A, and track width w. (e)–(h) Frequency for the main peak (f_1) as a function of D, K, A, and w.

the middle of DW [Figs. 3(c) and 3(e)]. Nevertheless, when D is $-1.2\ \mathrm{mJ/m^2}$, A_φ is around 10°, and a larger A_φ appears near the track boundary [Figs. 3(d) and 3(e)]. In addition to amplitude, the inhomogeneous precession of the moments in the DW is also characterized from different phases for the oscillation of φ at different DW positions. When D is $-0.05\ \mathrm{mJ/m^2}$, the phases of φ at two track boundaries are almost the same but opposite to that in the DW central [Fig. 3(c)]. Nevertheless, when D is $-1.2\ \mathrm{mJ/m^2}$, the phase shifts from one boundary to the other [Fig. 3(d)]. Figure 3(f) shows the frequency dependence of the spatial average of A_φ in the DW, and two peaks appear around 1.4 GHz and 4.4 GHz, which is consistent with the FFT results.

The position and strength for the FFT peaks can be manipulated by several parameters, including D, K, A, and track width w (Fig. 4). We have found that when D is $-0.2\ \mathrm{mJ/m^2}$ or smaller, the FFT peaks are quite weak (not shown). When D is $-1.0\ \mathrm{mJ/m^2}$ or larger, the FFT peaks are enhanced relatively due to the weakening of spectra background [Fig. 4(a)]. On the other hand, the increase in D leads to the red shift of the main peak in FFT [Fig. 4(e)]. On the contrary, increasing A and K lead to the blue shift of the main peak that is weakened with an enhancing background [Figs. 4(b), 4(c), 4(f), and 4(g)]. In addition to tuning the magnetic parameters, we also consider the influence of changing the track width on the characteristic peak. Widening the track shifts the main peak to a lower frequency [Figs. 4(d) and 4(h)]. In a magnetic system with DMI, enhancing DMI or reducing A and K gives rise to a noncollinear alignment of magnetic moments. In our recent work, it is also shown that widening the track width introduces an inhomogeneous structure of magnetic moments in the DW.[46] Therefore, it is concluded that the DW sway is attributed from the nonuniform precession that is originated from the inhomogeneous structure of the magnetic moments in the DW. Under very strong exchange coupling and anisotropy energy or weak DMI, the precession of magnetic moments in DW becomes uniform, resulting in the rising of the spectra background and the disappearance of the sway mode.

There is an intrinsic noncollinear alignment of magnetic moments across DW. On the other hand, the DMI-relevant edge effects also contribute to the complicated DW structure near the track edge.[46,47] Without considering the edge effects, the field-induced DW motion can be quantitatively studied using the CCM. The DW dynamics is depicted by the position q and the azimuthal angle φ for the moment in the central of DW, and the tilting angle β of the DW plane with a strong DMI.[25] The group of Thiele equations is expressed as

$$\frac{\alpha\cos\beta}{\Delta}\dot{q}+\dot{\varphi}=\frac{\pi\gamma_0 H_{SO}J\cos\varphi}{2}+\gamma_0 H_z, \tag{4}$$

$$\frac{\cos\beta}{\Delta}\dot{q}-\alpha\dot{\varphi}=\frac{\gamma_0\pi D\sin(\varphi-\beta)}{2\Delta M_s}-\frac{\gamma_0\mu_0 N_x M_s\sin[2(\varphi-\beta)]}{2}, \tag{5}$$

$$\frac{\pi^2\Delta\alpha\mu_0 M_s}{6\gamma_0}\left[\tan^2\beta+\left(\frac{w}{\pi\Delta}\right)^2\frac{1}{\cos^2\beta}\right]\dot{\beta}=-\Delta\mu_0 N_x M_s^2\sin[2(\varphi-\beta)]-\Delta\mu_0 N_x M_s^2\cos^2(\varphi-\beta)\tan\beta-\frac{4A}{\Delta}\tan\beta+\frac{\pi D\sin\varphi}{\cos\beta}. \tag{6}$$

In Eqs. (4)–(6), the parameters including γ_0, μ_0, N_x, Δ, w, and H_z are the gyromagnetic ratio of an electron, the permeability of vacuum, the demagnetization factor, the DW width, the track width, and the external alternating field along the z direction that is expressed as a sine function of time.

Based on Eqs. (4)–(6), an oscillation of β and φ under an out-of-plane alternating magnetic field is predicted, and the amplitude of β (A_β) decreases with increasing frequency (Fig. 5). This is accompanied with reducing amplitude of φ (A_φ) that is consistent well with the decaying background of spatial average of A_φ with frequency in the micromagnetic simulation. However, the appearance of characteristic peaks cannot be predicted by the CCM. This hints the importance of the DMI-relevant edge effects on the sway mode of the DW. Nevertheless, if edge effects are also considered, a precise quantitative analysis of DW dynamics by the CCM becomes quite challenging since the ansatz for initial DW is greatly destroyed after DW starts swaying. This is a typical nonlinear behavior that deserves further investigation.

In physics, the DMI-relevant edge effects depict the canting of moments at the track edge, satisfying the boundary condition (this is derived in the Appendix),[47]

$$\frac{d\vec{m}}{dn}=\frac{1}{\xi}(\vec{e}_z\times\vec{n})\times\vec{m}. \tag{7}$$

Here, $\xi=2A/D$. $\vec{m}$, $\vec{n}$, and $\vec{e}_z$ are the unit vectors for magnetization direction, normal direction at the track edge, and the out-of-plane direction of the film, respectively. We focus on $\vec{n}=\pm\vec{e}_y$ for the up and down edge in the y-axis direction, and Eq. (7) is converted into

$$\frac{d\vec{m}}{dy}=\pm\frac{1}{\xi}(\vec{e}_x\times\vec{m}). \tag{8}$$

Here, the ± sign is for $\vec{n}=\mp\vec{e}_y$.

Inside the track, the magnetic moments of DW rotate in the xz plane, while the DW moments at the track edge tilt toward y axis with an antisymmetric structure of moments at up and down edges (Fig. 6 in the Appendix). This leads to different initial states and effective field for the precession of moments at two edges and inner the track. On the other hand, the characteristic frequency for the moments at the track edge and inside the track is also quite

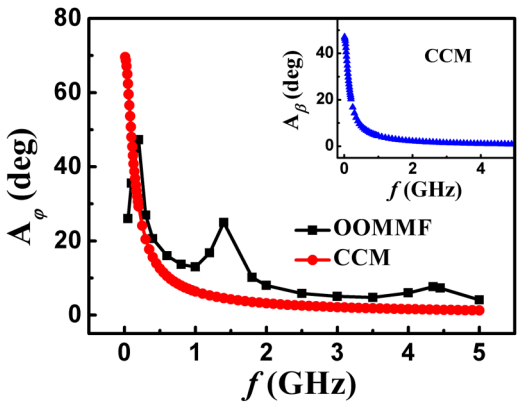

FIG. 5. Frequency spectra of spatial average amplitude of azimuthal angle (A_φ) obtained from the simulation and the CCM (inset shows the frequency dependence of the amplitude of tilting angle determined by the CCM).

different. As a result, under an alternating magnetic field, the DW moments at the track edge and inside precess at different phases and amplitudes. When DW deformation is considered, the coordinate for the central position of a DW is y dependent [$q(y, t)$]. Since the time dependence of q is correlated to the temporal azimuthal angle of the magnetic moment, the nonuniform precession of moments throughout the DW region results in a complicated y-dependent local DW velocity, which behaves as the sway of the DW.

CONCLUSION

In summary, the sway mode has been revealed numerically in the chiral DWs with strong DMI under an out-of-plane alternating magnetic field. The sway becomes outstanding at several characteristic frequencies, and it is originated from the DMI-relevant edge effects that introduce an inhomogeneous precession of the magnetic moments in the DW excited by an out-of-plane alternating magnetic field. The frequency can be well manipulated by the changing magnetic parameters and the track width. This work shows the importance of edge effects in studying the dynamics of the DW with a strong DMI in a nanotrack. Experimentally, the sway mode under an alternating magnetic field is expected to be detected via magnetoresistance measurements.[49]

SUPPLEMENTARY MATERIAL

The movies depicting the sway mode of chiral DW under an alternating magnetic field are given in the supplementary material.

ACKNOWLEDGMENTS

The authors would like to acknowledge the financial support from the National Natural Science Foundation of China (NNSFC) (Nos. 11574096, 61674062, and 61774001), the Natural Science Foundation of Hebei Province of China (Grant No. F2019202141), and the Huazhong University of Science and Technology (No. 2017KFYXJJ037).

APPENDIX: DERIVATION OF THE DMI-RELEVANT BOUNDARY CONDITION [EQ. (7)]

The free energy of interfacial DMI is expressed as the volume integration of the free energy density of DMI ($\varepsilon_{\mathrm{DMI}}$),

$$E_{\mathrm{DMI}} = \int_V \varepsilon_{\mathrm{DMI}}\, \mathrm{d}\tau, \tag{A1}$$

where $\varepsilon_{\mathrm{DMI}}$ is

$$\varepsilon_{\mathrm{DMI}} = D[\vec{m}\cdot\nabla m_z - (\nabla\cdot\vec{m})m_z]. \tag{A2}$$

The variation of E_{DMI} is

$$\delta E_{\mathrm{DMI}} = D\int_V [(\delta\vec{m})\cdot\nabla m_z + \vec{m}\cdot\nabla\delta m_z - (\nabla\cdot\delta\vec{m})m_z - (\nabla\cdot\vec{m})\delta m_z]\,\mathrm{d}\tau. \tag{A3}$$

This variation can be divided into two parts:

$$(\delta E_{\mathrm{DMI}})_1 = 2D\int_V [\nabla m_z - (\nabla\cdot\vec{m})\vec{e}_z]\cdot\delta\vec{m}\,\mathrm{d}\tau \tag{A4}$$

and

$$(\delta E_{\mathrm{DMI}})_2 = -D\int_V [(\delta\vec{m})\cdot\nabla m_z - (\nabla\cdot\vec{m})\delta m_z + (\nabla\cdot\delta\vec{m})m_z - \vec{m}\cdot\nabla\delta m_z]\,\mathrm{d}\tau. \tag{A5}$$

Based on Eq. (A4), we can define an effective magnetic field H_{eff} for DMI as

$$(\vec{H}_{\mathrm{eff}})_{\mathrm{DMI}} = \frac{2D}{\mu_0 M_S}[(\nabla\cdot\vec{m})\vec{e}_z - \nabla m_z]. \tag{A6}$$

This effective field decides the chirality of DW inside the track.

Using the Gauss formula, Eq. (A5) is converted into

$$\begin{aligned}(\delta E_{\mathrm{DMI}})_2 &= -D\int_S [m_z\delta\vec{m} - (\delta m_z)\vec{m}]\cdot\vec{n}\,\mathrm{d}\sigma \\ &= -D\int_S [(\vec{e}_z\times\vec{n})\times\vec{m}]\cdot\delta\vec{m}\,\mathrm{d}\sigma.\end{aligned} \tag{A7}$$

Here, $\vec{n}$ is the normal direction at the outside surface (S) of the region. Equation (A7) describes the contribution of DMI to the boundary condition.

In addition to DMI, exchange energy also contributes to the boundary condition. Using a similar method, the boundary

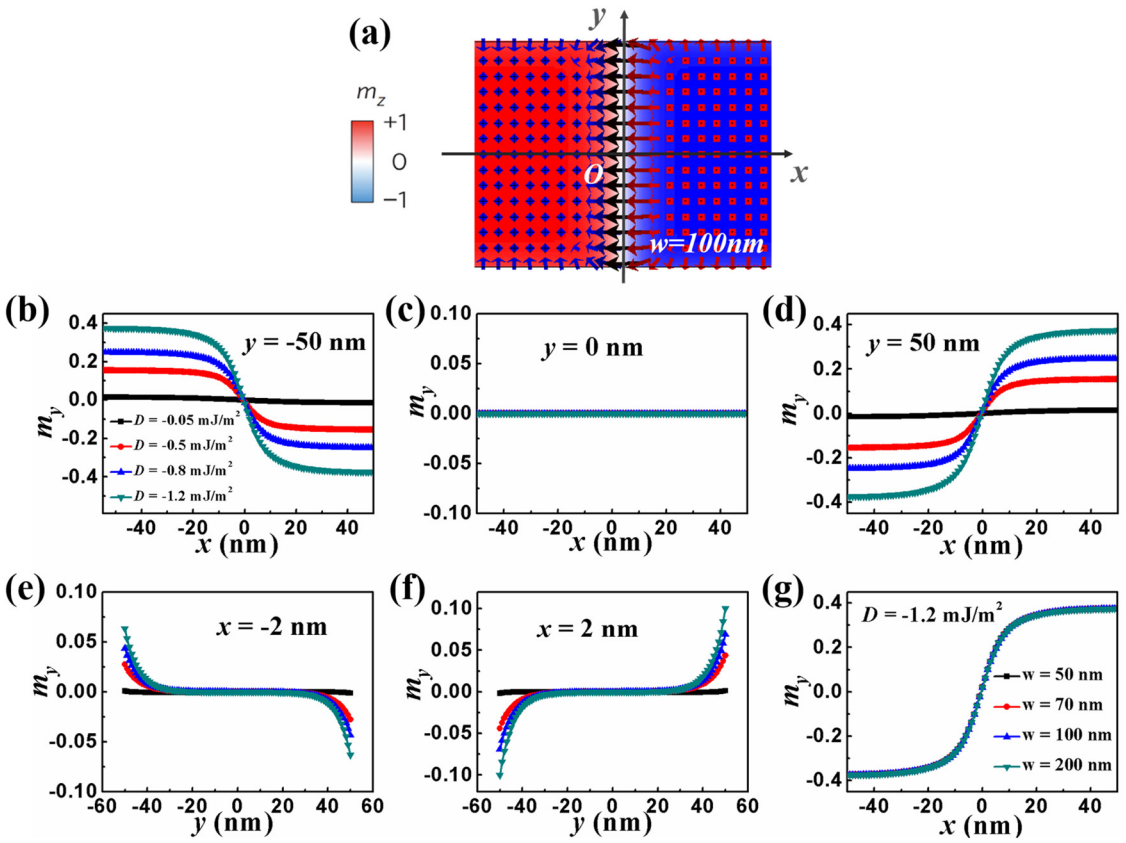

FIG. 6. (a) Snapshot of the structure of magnetic moments inside the track and at the track edge; (b) m_y as a function of x at $y = -50$ nm; (c) m_y as a function of x at $y = 0$ nm; (d) m_y as a function of x at $y = 50$ nm; (e) m_y as a function of y at $x = -2$ nm; (f) m_y as a function of x at $y = 2$ nm; (g) m_y as a function of x at $y = 50$ nm for different track widths.

condition from exchange energy is derived as

$$(\delta E_{ex})_2 = 2A \int_S \left(\frac{\partial \vec{m}}{\partial n}\right) \cdot \delta \vec{m}\, d\sigma. \tag{A8}$$

The total boundary condition comes from the following equation:

$$(\delta E_{DMI})_2 + (\delta E_{ex})_2 = 0. \tag{A9}$$

This equation needs to be satisfied for any surface. Therefore, it gives rise to

$$2A\frac{\partial \vec{m}}{\partial n} - D[(\vec{e}_z \times \vec{n}) \times \vec{m}] = 0. \tag{A10}$$

Equation (A10) depicts the total boundary condition.

Because of this boundary effect, the structure of the DW at the track edge is different from the one inside (Fig. 6). The local DW structure at one edge is antisymmetric to that at the other, and it is significantly different from that inside the track when the DMI is strong [Figs. 6(a)–6(d)]. This modification of the DW structure is concentrated near the track edge when the DMI is very small but is extended to the inner part with an increasing DMI [Figs. 6(e)–6(f)]. However, when the track width is 50 nm or larger, the DW structure at the edge does not change with the track width [Fig. 6(g)].

REFERENCES

[1]D. A. Allwood, G. Xiong, C. C. Faulkner, D. Atkinson, D. Petit, and R. P. Cowburn, Science **309**, 1688 (2005).
[2]D. Atkinson, D. A. Allwood, G. Xiong, M. D. Cooke, C. C. Faulkner, and R. P. Cowburn, Nat. Mater. **2**, 85 (2003).
[3]A. L. Dantas, M. S. Vasconcelos, and A. S. Carrico, J. Magn. Magn. Mater. **226-230**, 1604 (2001).
[4]U. Ebels, L. Buda, K. Ounadjela, and P. E. Wigen, Phys. Rev. B **63**, 174437 (2001).
[5]L. Berger, J. Appl. Phys. **55**, 1954 (1984).
[6]O. Boulle, J. Kimling, P. Warnicke, M. Kläui, U. Rüdiger, G. Malinowski, H. J. M. Swagten, B. Koopmans, C. Ulysse, and G. Faini, Phys. Rev. Lett. **101**, 216601 (2008).
[7]S. S. P. Parkin, M. Hayashi, and L. Thomas, Science **320**, 190 (2008).
[8]A. W. Rushforth, Appl. Phys. Lett. **104**, 162408 (2014).
[9]D. Claudio-Gonzalez, A. Thiaville, and J. Miltat, Phys. Rev. Lett. **108**, 227208 (2012).

[10]M. Hayashi, L. Thomas, R. Moriya, C. Rettner, and S. S. P. Parkin, Science **320**, 209 (2008).
[11]R. Moriya, L. Thomas, M. Hayashi, Y. B. Bazaliy, C. Rettner, and S. S. P. Parkin, Nat. Phys. **4**, 368 (2008).
[12]E. Saitoh, H. Miyajima, T. Yamaoka, and G. Tatara, Nature **432**, 203 (2004).
[13]L. Thomas, M. Hayashi, X. Jiang, R. Moriya, C. Rettner, and S. S. P. Parkin, Nature **443**, 197 (2006).
[14]O. A. Tretiakov and Ar. Abanov, Phys. Rev. Lett. **105**, 157201 (2010).
[15]J. Yu, X. Qiu, Y. Wu, J. Yoon, P. Deorani, J. M. Besbas, A. Manchon, and H. Yang, Sci. Rep. **6**, 32629 (2016).
[16]P. P. J. Haazen, E. Murè, J. H. Franken, R. Lavrijsen, H. J. M. Swagten, and B. Koopmans, Nat. Mater. **12**, 299 (2013).
[17]K.-S. Ryu, L. Thomas, S.-H. Yang, and S. Parkin, Nat. Nanotech. **8**, 527 (2013).
[18]S. Emori, U. Bauer, S. M. Ahn, E. Martinez, and G. S. D. Beach, Nat. Mater. **12**, 611 (2013).
[19]J. H. Franken, M. Herps, H. J. Swagten, and B. Koopmans, Sci. Rep. **4**, 5248 (2015).
[20]E. Martinez, S. Emori, and G. S. D. Beach, Appl. Phys. Lett. **103**, 072406 (2013).
[21]Y. Zhang, S. Luo, X. Yang, and C. Yang, Sci. Rep. **7**, 2047 (2017).
[22]S. Emori, E. Martinez, K.-J. Lee, H.-W. Lee, U. Bauer, S.-M. Ahn, P. Agrawal, D. C. Bono, and G. S. D. Beach, Phys. Rev. B **90**, 184427 (2014).
[23]E. Martinez, S. Emori, N. Perez, L. Torres, and G. S. D. Beach, J. Appl. Phys. **115**, 213909 (2014).
[24]K.-S. Ryu, L. Thomas, S.-H. Yang, and S. S. P. Parkin, Appl. Phys. Express **5**, 093006 (2012).
[25]O. Boulle, S. Rohart, L. D. Buda-Prejbeanu, E. Jué, I. M. Miron, S. Pizzini, J. Vogel, G. Gaudin, and A. Thiaville, Phys. Rev. Lett. **111**, 217203 (2013).
[26]E. Jué, A. Thiaville, S. Pizzini, J. Miltat, J. Sampaio, L. D. Buda-Prejbeanu, S. Rohart, J. Vogel, M. Bonfim, O. Boulle, S. Auffret, I. M. Miron, and G. Gaudin, Phys. Rev. B **93**, 014403 (2016).
[27]S. A. Nasseri, B. Sarma, G. Durin, and C. Serpico, Phys. Proc. **75**, 974 (2015).
[28]A. J. Schellekens, A. van den Brink, J. H. Franken, H. J. M. Swagten, and B. Koopmans, Nat. Commun. **3**, 847 (2012).
[29]W. Lin, N. Vernier, G. Agnus, K. Garcia, B. Ocker, W. Zhao, E. E. Fullerton, and D. Ravelosona, Nat. Commun. **7**, 13532 (2016).
[30]T. Koyama, Y. Nakatani, J. Ieda, and D. Chiba, Sci. Adv. **4**, eaav0265 (2018).
[31]C. Ma, X. Zhang, J. Xia, M. Ezawa, W. Jiang, T. Ono, S. N. Piramanayagam, A. Morisako, Y. Zhou, and X. Liu, Nano Lett. **19**, 353 (2019).
[32]P. Yan, X. S. Wang, and X. R. Wang, Phys. Rev. Lett. **107**, 177207 (2011).
[33]X.-G. Wang, G.-H. Guo, Y.-Z. Nie, G.-F. Zhang, and Z.-X. Li, Phys. Rev. B **86**, 054445 (2012).
[34]D. Hinzke and U. Nowak, Phys. Rev. Lett. **107**, 027205 (2011).
[35]J. Lan, W. Yu, R. Wu, and J. Xiao, Phys. Rev. X **5**, 041049 (2015).
[36]D.-S. Han, S.-K. Kim, J.-Y. Lee, S. J. Hermsdoerfer, H. Schultheiss, B. Leven, and B. Hillebrands, Appl. Phys. Lett. **94**, 112502 (2009).
[37]W. Wang, M. Albert, M. Beg, M.-A. Bisotti, D. Chernyshenko, D. Cortés-Ortuño, I. Hawke, and H. Fangohr, Phys. Rev. Lett. **114**, 087203 (2015).
[38]S.-H. Yang and S. Parkin, J. Phys. Condens. Matter **29**, 303001 (2017).
[39]I. M. Miron, T. Moore, H. Szambolics, L. D. Buda-Prejbeanu, S. Auffret, B. Rodmacq, S. Pizzini, J. Vogel, M. Bonfim, A. Schuhl, and G. Gaudin, Nat. Mater. **10**, 419 (2011).
[40]A. Thiaville, S. Rohart, É Jué, V. Cros, and A. Fert, EPL **100**, 57002 (2012).
[41]D. J. Clarke, O. A. Tretiakov, G.-W. Chern, Y. B. Bazaliy, and O. Tchernyshyov, Phys. Rev. B **78**, 134412 (2008).
[42]O. A. Tretiakov, D. Clarke, G.-W. Chern, Ya. B. Bazaliy, and O. Tchernyshyov, Phys. Rev. Lett. **100**, 127204 (2008).
[43]V. V. Slastikov, C. B. Muratov, J. M. Robbins, and O. A. Tretiakov, Phys. Rev. B **99**, 100403(R) (2019).
[44]C. B. Muratov, V. V. Slastikov, A. G. Kolesnikov, and O. A. Tretiakov, Phys. Rev. B **96**, 134417 (2017).
[45]D. Y. Kim, M. H. Park, Y. K. Park, J. S. Kim, Y. S. Nam, H. S. Hwang, D. H. Kim, S. G. Je, B. C. Min, and S. B. Choe, Phys. Rev. B **97**, 134407 (2018).
[46]M. Shen, Y. Zhang, W. Luo, L. You, and X. Yang, J. Magn. Magn. Mater. **485**, 69 (2019).
[47]S. Rohart and A. Thiaville, Phys. Rev. B **88**, 184422 (2013).
[48]M. Beg, M. Albert, M.-A. Bisotti, D. Cortés-Ortuño, W. Wang, R. Carey, M. Vousden, O. Hovorka, C. Ciccarelli, C. S. Spencer, C. H. Marrows, and H. Fangohr, Phys. Rev. B **95**, 014433 (2017).
[49]W. Lin, J. Cucchiara, C. Berthelot, T. Hauet, Y. Henry, J. A. Katine, E. E. Fullerton, and S. Mangin, Appl. Phys. Lett. **96**, 252503 (2010).